1-1-2024

Economic material for large-scale H2 storage and H2-CO2 separation

Hussein R. Abid
Edith Cowan University

Alireza Keshavarz
Edith Cowan University

Header Jaffer

Basim K. Nile

Stefan Iglauer
Edith Cowan University

10.1016/j.est.2023.109770
Abid, H. R., Keshavarz, A., Jaffer, H., Nile, B. K., & Iglauer, S. (2024). Economic material for large-scale H2 storage and H2-CO2 separation. Journal of Energy Storage, 75, article 109770. https://doi.org/10.1016/j.est.2023.109770

Journal of Energy Storage 75 (2024) 109770

Contents lists available at ScienceDirect

Journal of Energy Storage

journal homepage: www.elsevier.com/locate/est

Research papers

Economic material for large-scale H_2 Storage and H_2-CO_2 separation

Hussein Rasool Abid [a,b,*], Alireza Keshavarz [a], Header Jaffer [c], Basim K. Nile [d], Stefan Iglauer [a,**]

[a] Centre for Sustainable Energy and Resources, Edith Cowan University, 270 Joondalup Dr, Joondalup 6027, WA, Australia
[b] Environmental Health Department, Applied Medical Sciences, University of Kerbala, Karbala 56001, Iraq
[c] Physiology and Medical Physics Department, College of Medicine, University of Kerbala, 56001, Iraq
[d] Civil Engineering Department, College of Engineering, University of Kerbala, Karbala 56001, Iraq

ARTICLE INFO

Keywords:
H_2 adsorption
CO_2 adsorption
Selectivity (CO_2/H_2)
Methyl orange
Sub-bituminous coal

ABSTRACT

Hydrogen is a clean fuel that can potentially completely decarbonize the energy supply chain and mitigate global warming. Hydrogen – a highly volatile gas – however, needs to be separated from CO_2 during H_2 production, and also from cushion gas in H_2 geo-storage projects; in addition, large-scale H_2 storage is a key obstacle. We thus tested and chemically upgraded common sub-bituminous coal as a material for H_2-CO_2 separation and H_2 storage.

The coal adsorbed significant amounts of H_2 and CO_2 and demonstrated an excellent H_2-CO_2 separation efficiency if chemically modified. The work presented here thus provides fundamental data required for the economic production and storage of H_2, so that an industrial-scale clean and sustainable energy supply can be established.

1. Introduction

Globing warming is increasingly affecting our climate in a detrimental way. Greenhouse gas emissions must thus be drastically reduced and associated clean and sustainable energy supplies need to be established [1,2].

CO_2 is the foremost gas emitted into the atmosphere when fossil fuels are burned; therefore, many techniques have been used to control its emission [3]. Carbon capture utilization and storage (CCUS) technologies are specifically used to reduce CO_2 emissions [4]. The post-combustion techniques (Absorption, adsorption, and membrane) are worldwide used to capture CO_2 after occurring the combustion [5]. The adsorption technique based on the use of solid porous materials (adsorbents) is popularly utilized to capture or separate CO_2 [6]. Although the adsorption process can offer notable energy savings in comparison with other methods, this process has some drawbacks related to its performance and efficiency in the removal of CO_2 [7]. However, the best solution is to use zero-carbon emission fuel, therefore, hydrogen is the global candidate to replace conventional fossil fuels [8].

In this context, a hydrogen (H_2)-based economy, but also carbon capture and storage (CCS – typically combined with fossil fuel burning) solutions have been proposed, and, to a rather limited extent, implemented [9]. Two main obstacles exist in this respect, namely firstly, how to store the highly compressible H_2 and the very large quantities of CO_2 (>50 Gt/a) [10], and secondly, how to separate H_2 from CO_2 (which is required after producing H_2 via steam reforming or when H_2 has to be separated from cushion gas in underground hydrogen storage) [11–14]. Various materials have been used to capture and separate gases [15]. Modification process was effectively used to improve the adsorption affinities of some adsorbents, enhancing their storage capacities for CO_2 and H_2 and their separation [16,17]. Coal is the cheapest material that is hugely available, therefore it was considered to be an excellent alternative adsorbent instead of commercial ones. Sub-bituminous coal was successfully tested for H_2 adsorption with a competitive adsorption potential [13]. Also, this coal was chemically modified and utilized as a promising material for CO_2 storage and CO_2-H_2 separation, which was unprecedentedly enhanced in modified –coal [16]. Huge amount of dyes is discharged into rivers as wastewater, therefore removing of this waste is an essential request to protect the public health and environment. Many techniques are used to remove cationic and anionic dyes from wastewater [18]. However, due to the chemical and electronic characteristics of the dyes, anionic dyes such as Congo red (CR), Xylenol orange (XO), Methyl orange (MO) and Bromothymol blue (BB) have been recently used to change the surface

* Correspondence to: H.R. Abid, Environmental Health Department, Applied Medical Sciences, University of Kerbala, Karbala 56001, Iraq.
** Corresponding author.
E-mail addresses: hussein.r@uokerbala.edu.iq (H.R. Abid), s.iglauer@ecu.edu.au (S. Iglauer).

https://doi.org/10.1016/j.est.2023.109770
Received 15 August 2023; Received in revised form 10 November 2023; Accepted 14 November 2023
Available online 18 November 2023

Table 1
Chemical properties of the sub-bituminous coal used here [21].

Approximate analysis			
Moisture content wt %	Ash content wt %	Volatile content wt %	Fixed carbon wt %
21.1	2.5	28.0	47.8

Petrographic analysis			
Vitrinite vol%	Liptinite vol%	Inertinite vol%	Mineral matter vol%
33.3	11.3	43.9	11.5

Ultimate analysis			
Carbon wt%	Hydrogen wt%	Nitrogen wt%	Relative density
58.1	2.98	1.15	1.39

functionalities of adsorbents toward enhancing CO_2 adsorption [19–21]. Accordingly, the injection of the dyes in the coal reservoirs is expected to dually work; firstly, to discard the waste of the dyes and secondly to improve their implication for gas storage.

We, therefore, tested, modified, and chemically improved common sub-bituminous coal in terms of its gas adsorption (gas storage) and gas separation (separation efficiency) capabilities. We demonstrate that coal can adsorb large amounts of CO_2, but also significant amounts of H_2; the coals – especially the chemically improved ones – also showed excellent H_2-CO_2 separation efficiencies. This work thus provides fundamental data for a novel gas storage and separation process, and aids in the implementation of a fully decarbonized energy supply chain.

2. Materials and methods

2.1. Coal material

A sub-bituminous coal sample (Pan Upper; Collie, Western Australia) with a maximum vitrinite reflectance of 0.38 % was crushed and sieved to a homogenous particle size (250–450 μm). Ultimate and proximate analysis were previously performed on the same coal, compare Table 1.

2.2. Modification of coals

Sub-bituminous coal was modified with methyl orange (MO, dye content 85 wt%). Thus 25 and 100 ppm aqueous methyl orange solutions were prepared (at 303 K and pH 7) by adding 1 g of the raw coal into 40 mL of deionized (DI) water under ongoing mixing for 2 days. Subsequently, the resulting coal-MO powder was separated from the

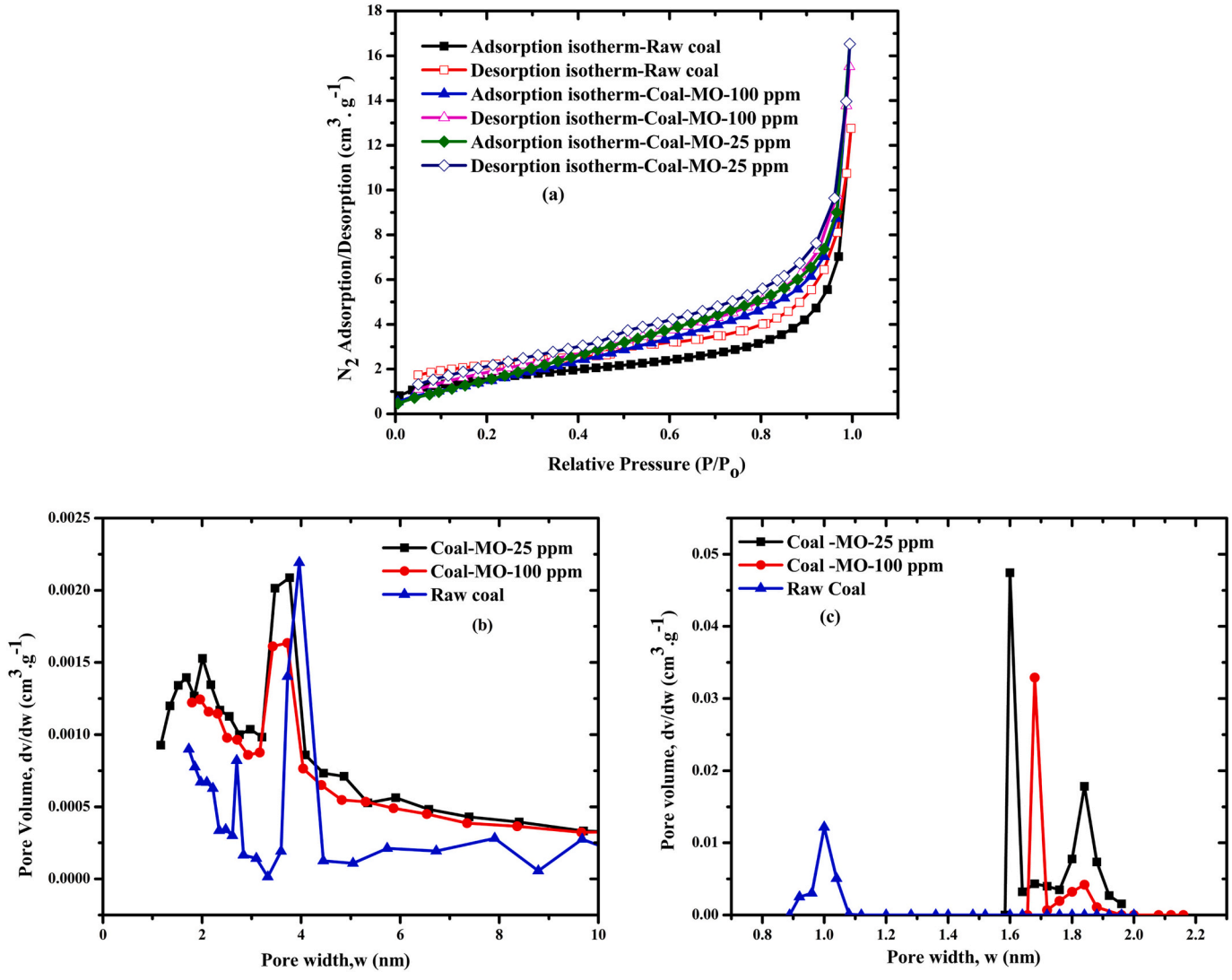

Fig. 1. N_2 Adsorption/desorption isotherms (a); and mesopore (b) and micropore (c) size distributions measured for the tested coals.

Table 2
Textural properties of the coals examined.

Coal	BET surface area (m^2/g)	Total pore volume (cm^3/g)	Average micropore diameter (nm)[a]	Average pore diameter (nm)[a]
Raw coal	5.78	0.027	2.23	14.45
Coal-MO-25 ppm	6.45	0.025	1.73	15.85
Coal-MO-100 ppm	6.88	0.024	1.2	14.00

[a] Arithmetic average from BET analysis.

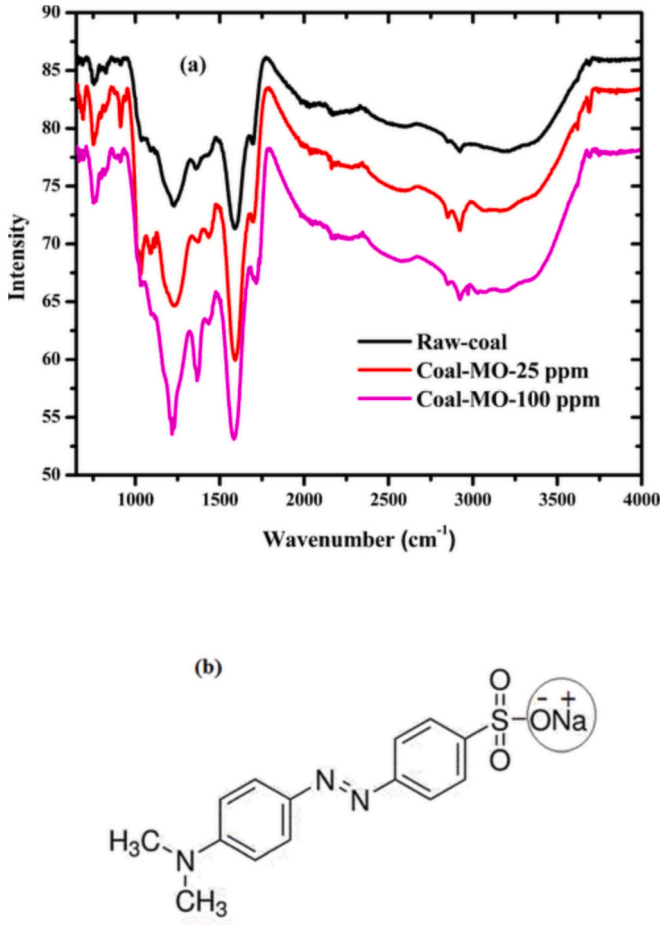

Fig. 2. FTIR spectra of raw and treated coals (a) and chemical structure of MO (b).

dispersions via vacuum filtration using filter paper grade 1 (11 μm openings), and the MO-coal powder was dried at 343 K for 24 h in a preheated oven. Note that the raw coal used was washed with deionized water prior to use.

2.3. Coal characterization

The prepared coal samples were thoroughly analysed via a range of techniques, including ATR-FTIR (using a Perkin Elmer Spectrometer 100-FT-IR), N_2 adsorption/desorption isotherms and pore size distribution (PSD) measurements (using a Tristar 3020 instrument), Powder X-ray diffraction (PXRD) using a RAYONS X-Rays instrument (with a cobalt K_α radiation source at 40 kV and 40 mA and phase identification via High Score software) as well as SEM imaging and EDS mapping (performed with a Hitachi SU3500 Scanning Electron Microscope).

2.4. Adsorption measurements

CO_2 (HPG, purity ≥99.99 mol%), H_2 (Grade 5.0; UHPG, purity ≥99.999 mol%), He (HPG, purity ≥99.99 mol%) and Air (Instrument Grade-Compressed, purity ≥99.99 mol%) were supplied by Coregas. Static adsorption was measured on a PCTpro adsorption analyzer (SETARAM Instrumentation) as described earlier [21]. All adsorption tests were performed at prescribed pressures (7–42 bar) at 303 K. Several tests were repeated thrice, and the average standard deviation was estimated as 2.4 % based on these replicate measurements.

3. Results and discussion

3.1. Characterization of the raw and modified coals

All N_2 adsorption/desorption isotherms demonstrated desorption hysteresis, indicating type IV adsorption systems, Fig. 1a. Note that in a type IV adsorption systems, mesopores (2 nm – 50 nm) and macropores (>50 nm) dominate [22,23]. This hysteresis was narrower in the coal-MO samples due to the modification of the pore network (caused by MO incorporation) [24,25]. Incorporation of MO into the coal matrix also changed the PSD and the textural properties of the modified samples.

Specifically, BET surface area increased with increasing MO content. Furthermore, the coal-MO samples demonstrated higher microporosities than the raw coal, therefore, in contrast to average pore diameter, the average micropore was decreased with increasing the content of MO, Table 2. Whereas, Fig. 1b (mesopore size distribution) shows that, mesopore diameter decreased mainly from 4 nm in raw coal to 3.5 nm in both coal-MO samples and micropore diameter in Fig. 1c (micropore size distribution) increased from 1 nm in raw coal to 1.6 and 1.9 nm in coal-MO-25 ppm, and 1.7 nm in coal-MO-100 ppm.

MO incorporation into the coal was also confirmed by FTIR, and a slight shift in FTIR signals was observed for the treated samples, Fig. 2a. Thus MO functionalities increased the intensities of some peaks, including the broad band at wavenumber 3250 cm^{-1} (caused by O—H stretching vibrations) [26], the peaks at 2850 and 2923 cm^{-1} (C—N bond vibrations, and/or asymmetric CH_3 stretching vibrations) [27], the peak at 1698 cm^{-1} (C═O stretching vibrations) [28,29], the peaks at 1373 and 1434 cm^{-1} (N═N stretching vibrations), the peaks at 1229 and 1592 cm^{-1} (CH_3 and C═C stretching vibrations), the peaks at 685 and 755 cm^{-1} (C—S stretching vibrations), as well as the peaks at 913, 1032, and 1091 cm^{-1} (SO_3 stretching vibrations).

In addition, with increasing MO concentration, the sodium (Na) content increased, compare EDS images in Fig. 3. This increase in Na concentration in the modified samples is stemming from the incorporation of MO into the coal as MO contained Na, see Fig. 3b.

XRD peak patterns overlapped, albeit their peak intensities varied between the samples, Fig. 4. This shift in XRD-peak intensities was caused by the changing kaolinite content, while the quartz content was reduced proportionally (e.g. an additional peak emerged at $2\theta = 36.98°$ for coal-MO-100 ppm, Fig. 5, this peak is one of the main kaolinite peaks [30]) (Table 3).

3.2. H_2 and CO_2 adsorption capacities

3.2.1. H_2 adsorption capacities

H_2 adsorption capacity $\kappa(H_2)$ significantly decreased when MO was incorporated into the coal, Fig. 5a. Thus, $\kappa(H_2)$ decreased from 0.24 mol/kg coal for raw sub-bituminous coal to 0.172 mol/kg for 25 ppm MO-coal and 0.058 mol/kg for 100 ppm MO (at 323 K and 42.5 bar); this reduction can be attributed to MO molecules being not uniformly incorporated into the coal as the coal is not a homogenous matrix [31].

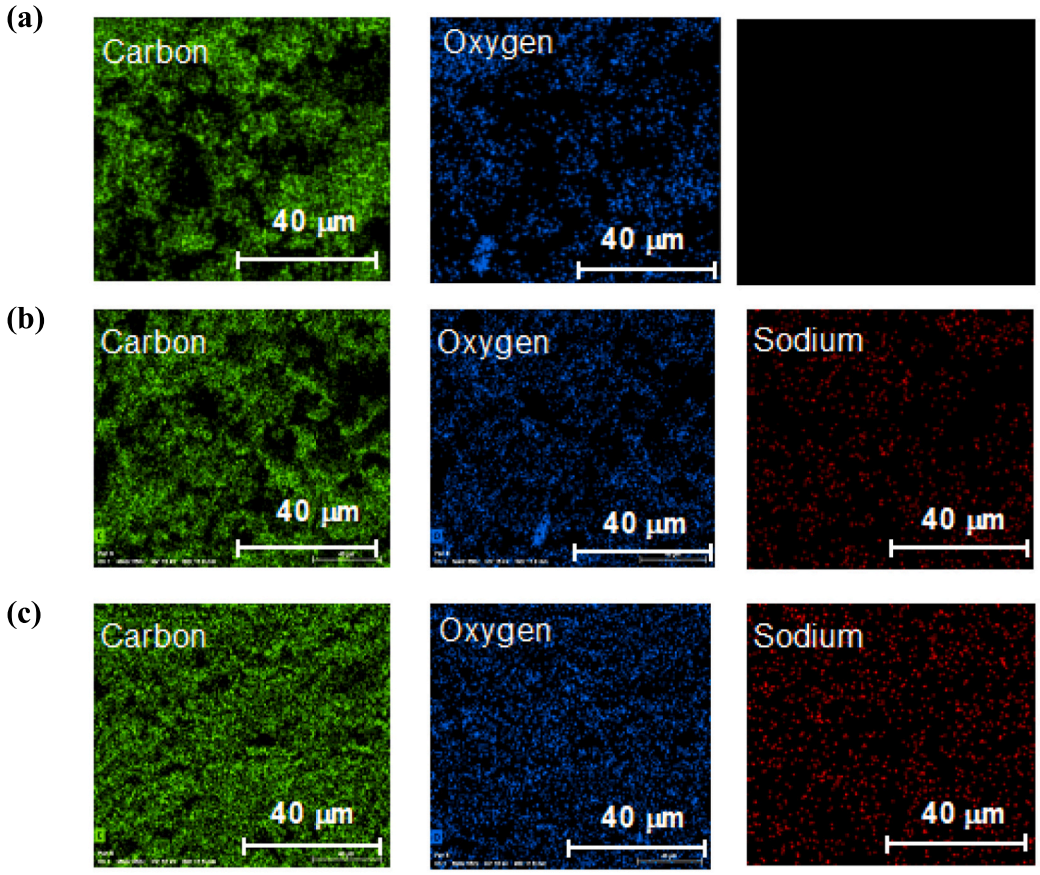

Fig. 3. Energy-dispersive x-ray spectrographic maps of carbon (C), oxygen (O) and sodium (Na) on a) raw coal, b) coal-MO-25 ppm and c) coal-MO-100 ppm.

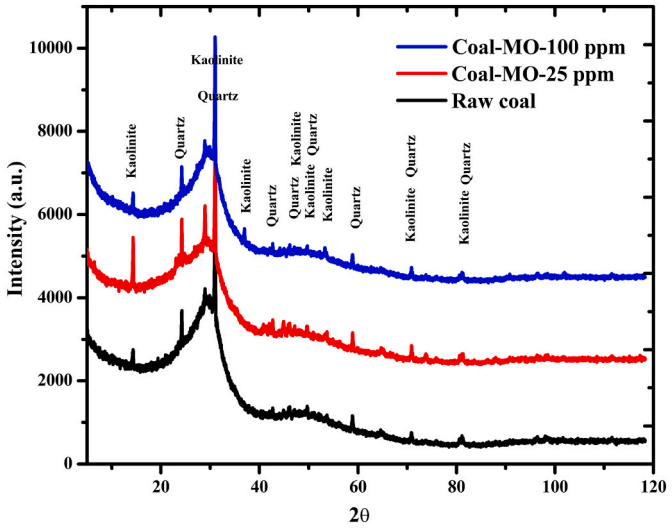

Fig. 4. XRD patterns of the coals tested.

Note that orbital interactions (induced by polarization of H_2 molecules) are more dominant in adsorbents enriched with functional groups which contain free electrons (e.g. amine or carbonyl groups) [14,32]. Hence, the negative charge on one end and the dimethyl substituted nitrogen atom on the other end of the MO molecule induced weak interactions with hydrogen species [33]; however, as MO (and consequently the negative MO charges) were randomly distributed on the surfaces of modified coals, H_2 polarization and thus H_2 adsorption were reduced. [34–36].

The $\kappa(H_2)$ response to increasing pressure, was, however, more complex. While at highest MO loading (100 ppm), $\kappa(H_2)$ increased monotonically with pressure on raw coal, $\kappa(H_2)$ for the MO-100 ppm and the MO-25 ppm coal exhibited a non-linear response, and $\kappa(H_2)$ went through a maximum (at ~35 bar). This non-linear response was caused by two opposing factors, namely a) the increase in $\kappa(H_2)$ with increasing pressure [13], and b) the decrease in pore accessibility due to the compression of the pores at high pressure.

3.2.2. CO_2 adsorption capacities

CO_2 adsorption capacity ($\kappa(CO_2)$) strongly increased with MO incorporation, Fig. 5b; specifically, $\kappa(CO_2)$ increased from 2.15 mol/kg in raw coal to 3.6 and 5.25 mol/kg in coal-MO-25 ppm and coal-MO-100 ppm. This was caused by electron-rich functional surface groups (such as -OH, C═O, -SO_3, N═N and C═C, compare Fig. 3), which were more concentrated on the MO-modified coal surfaces.

This increase in negative surface charge density (induced by these electron-rich functional groups) strongly attracted CO_2 molecules (due to CO_2's high quadrupole moment) [14,32], leading to increased CO_2 adsorption. Specifically, an increase in CO_2 adsorption was due to encapsulation of the anionic MO into the coal pores. This encapsulated negative charge dyes enhanced the polarity of the pores and strongly attracted positive moieties of the CO_2 molecules and consequently oriented the adsorbed CO_2 molecules parallel to the adsorbent's surface [20,21]. This flat adsorption profile significantly enhances CO_2–CO_2 intermolecular interaction and reducing the steric hindrance caused by perpendicular orientation of CO_2 within the adsorption film inside the pores. The orientation is usually driven by the chemical nature of the pore wall and the strength of CO_2-surface interactions. The adsorption capacity was also further enhanced with slightly increasing the surface

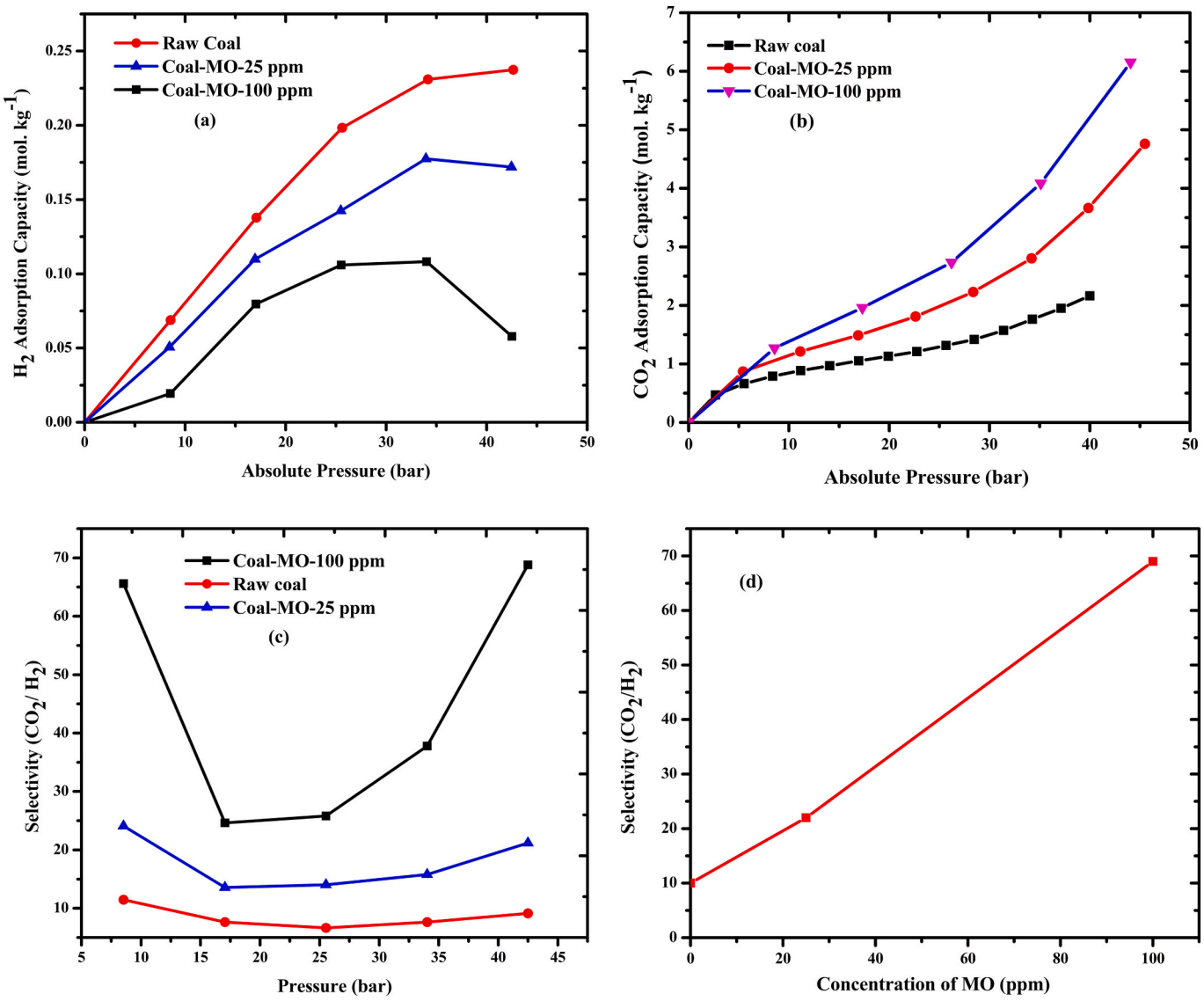

Fig. 5. Adsorption isotherms of (a) H_2 and (b) CO_2 as a function of pressure (measured at 323 K), and CO_2-H_2 separation factor as a function of pressure (c) and MO concentration (d).

Table 3
Composition of mineral the coals tested (based on XRD analysis).

Coal	Quartz (wt%)	Kaolinite (wt%)
Sub-bituminous	56	44
Sub-bituminous-25	35	65
Sub-bituminous-100	31	69

area and reducing the pore size in the coal-MO samples [21,37].

Moreover, $\kappa(CO_2)$ increased drastically and monotonically with increasing pressure, Fig. 5b. This is consistent with previous results on a large range of coal/coal ranks [38]. Again, the increased molecular CO_2 concentration at increased pressure led to stronger CO_2-coal affinity and thus higher CO_2 adsorption [21,39]. Finally, $\kappa(CO_2)$ was much higher than $\kappa(H_2)$ (e.g. $\kappa(CO_2)$) at 30 bar and 323 K was 0.11–0.21 mol/kg for H_2, while it was 1.5–3.7 mol/kg for CO_2 (caused by the much higher CO_2 quadrupole moment [32]). Thus, we also conclude that steric hindrance effect observed for H_2 adsorption was insignificant in terms of CO_2 adsorption.

3.3. CO_2/H_2 separation factor

CO_2 separation from a CO_2/H_2 mixture can be performed via preferential adsorption (if one gas has a higher adsorption capacity than the other); the efficiency of this process can be quantified by the CO_2/H_2 separation factor Ω ($= \kappa_{CO2}/\kappa_{H2}$; a specific value for a given thermophysical condition). Here, for the coals examined, Ω reached a high value (2–69), depending on pressure and coal type; this is discussed in more detail below.

3.3.1. Effect of methyl orange on CO_2/H_2 separation factor

Ω drastically increased when MO was incorporated (compare Ω = 2–12 for raw coal with Ω = 15–25 for MO-25 ppm coal and Ω = 27–69 for MO-100 ppm coal, Fig. 5). All Ω-pressure curves (for all three coals tested) demonstrated a minimum at intermediate pressures (at 15–35 bar); these minima appeared at lower pressures when MO was incorporated (15–25 bar for MO-coal versus 22–30 bar for raw coal, Fig. 5c and d). Very high Ω values (~70) could be achieved with MO-100 ppm coal at relatively low (<10 bar) pressures but also at high pressures (>40 bar); such Ω-values are comparable to those of MOF [40], zeolites [41] and activated carbon [42] adsorbents. As such commercial

Table 4
CO_2 and H_2 adsorption and theoretical CO_2/H_2 selectivity.

Adsorbent	Temperature K	Pressure bar	$C0_2$ mmol/g	H_2 mmol/g	Selectivity CO_2/H_2	References
NOTT-101/OEt	313	20	14	1.2	11.6	[44]
T-MOF-5	298	23	15.22	0.61	24	[40]
HKUST-1	303	20	4	0.25	16	[45]
BeBTB	313	30	27	5	5.4	[46]
ZIF-8	333	30	7	0.25	28	[47]
Carbonate-2	333	20	0.4	0.2	2	[48]
Zeolite NaY	308	7.5	6.7	0.13	51.5	[41]
Zeolite –X13	298	10	6.35	0.22	28	[49]
Activated carbon	303	20	7.6	0.52	14.62	[42]
Activated carbon-GCN	308	7.5	6.2	0.2	31	[41]
Activated carbon	298	20	8.8	2	4	[50]
MCM-41	298	20	8	0.45	17.7	[51]
Coal-MO-100 ppm	323	20	2.25	0.09	25	Current work
Coal-MO-25 ppm	323	20	1.6	0.12	13.33	Current work
Raw coal	323	20	1.2	0.16	7.5	Current work

adsorbents are much more expensive than coal [43], MO-coals might be a good economic alternative. Table 4 shows the adsorption capacity of CO_2 and H_2 as pure component gases and the theoretical calculated selectivity of CO_2/H_2 in different adsorbents compared with the adsorbents used in this study. It is obviously noticed that although MOF, zeolites and activated carbons have very high specific surface areas, coal-MO-100 ppm at 20 bar and 323 K exposed a distinguished selectivity among other adsorbents. For instance, selectivity of CO_2/H_2 in coal-MO-100 ppm was around double that in NOTT-110/OET (BET, 2023 $m^2.g^{-1}$) and equivalent to that in T-MOF-5 (BET, 1280 $m^2.g^{-1}$). Consequently, anionic MO modification significantly and chemically improved the nature of the pore surfaces in the coals, achieving unbelievable enhancement in the CO_2 adsorption.

4. Conclusions

H_2 storage and H_2 separation from CO_2/H_2 streams are required for the large-scale implementation of a decarbonized energy supply chain. We thus identified, tested, and further upgraded an economic material (common sub-bituminous coal) in terms of its H_2 storage and separation efficiencies. Clearly, very high H_2-CO_2 separation efficiencies (κ = 60–70) could be achieved with MO-100 ppm modified coal, comparable to that of (the much more expensive) MOFs ($\kappa \sim 65$). The coal was also a good adsorbent for H_2 and CO_2; coal can thus in principle also act as a gas storage material. The work presented here provides fundamental data related to the production and storage of H_2 and thus aids in the implementation of a full-scale clean energy supply chain.

CRediT authorship contribution statement

Hussein Rasool Abid: Conceptualization, Methodology, Experimental Work, Writing the First Draft, Visualization. **Alireza Keshavarz**: Conceptualization, Review & Editing.

Header Jaffer: Review & Editing. **Basim K. Nile**: Review& Editing. **Stefan Iglauer**: Methodology, Writing - Review & Editing.

Declaration of competing interest

The authors declare that they have no known competing financial interests or personal relationships that could have appeared to influence the work reported in this paper.

Data availability

Data will be made available on request.

Acknowledgements

We would like to acknowledge funding support from the Australian Research Council (grant DP220102907).

References

[1] N. Stern, J. Rydge, The new energy-industrial revolution and international agreement on climate change, Econ. Energy Environ. Policy 1 (2012) 101–120.
[2] H.D. Matthews, S. Wynes, Current global efforts are insufficient to limit warming to 1.5 C, Science 376 (2022) 1404–1409.
[3] A. Mualim, H. Huda, A. Altway, J.P. Sutikno, R. Handogo, Evaluation of multiple time carbon capture and storage network with capital-carbon trade-off, J. Clean. Prod. 291 (2021) 125710.
[4] K. Jiang, P. Ashworth, S. Zhang, X. Liang, Y. Sun, D. Angus, China's carbon capture, utilization and storage (CCUS) policy: a critical review, Renew. Sust. Energ. Rev. 119 (2020) 109601.
[5] C. Chao, Y. Deng, R. Dewil, J. Baeyens, X. Fan, Post-combustion carbon capture, Renew. Sust. Energ. Rev. 138 (2021) 110490.
[6] A. Allangawi, E.F.H. Alzaimoor, H.H. Shanaah, H.A. Mohammed, H. Saqer, A.A. El-Fattah, A.H. Kamel, Carbon capture materials in post-combustion: adsorption and absorption-based processes, C 9 (2023) 17.
[7] F. Raganati, F. Miccio, P. Ammendola, Adsorption of carbon dioxide for post-combustion capture: a review, Energy Fuel 35 (2021) 12845–12868.
[8] A. Alzoubi, Renewable Green hydrogen energy impact on sustainability performance, Int. J. Comput. Inf. Manuf. 1 (2021).
[9] Y. Jiang, P.M. Mathias, R.F. Zheng, C.J. Freeman, D. Barpaga, D. Malhotra, P. K. Koech, A. Zwoster, D.J. Heldebrant, Energy-effective and low-cost carbon capture from point-sources enabled by water-lean solvents, J. Clean. Prod. 388 (2023) 135696.
[10] H.-O. Pörtner, D.C. Roberts, H. Adams, C. Adler, P. Aldunce, E. Ali, R.A. Begum, R. Betts, R.B. Kerr, R. Biesbroek, Climate change 2022: impacts, adaptation and vulnerability, in: IPCC Sixth Assessment Report, 2022, pp. 37–118.
[11] M. Kanaani, B. Sedaee, M. Asadian-Pakfar, Role of cushion gas on underground hydrogen storage in depleted oil reservoirs, J. Energy Storage 45 (2022) 103783.
[12] J. Graetz, New approaches to hydrogen storage, Chem. Soc. Rev. 38 (2009) 73–82.
[13] S. Iglauer, H. Abid, A. Al-Yaseri, A. Keshavarz, Hydrogen adsorption on sub-bituminous coal: implications for hydrogen geo-storage, Geophys. Res. Lett. 48 (2021), e2021GL092976.
[14] H.R. Abid, A. Keshavarz, J. Lercher, S. Iglauer, Promising material for large-scale H2 storage and efficient H_2-CO_2 separation, Sep. Purif. Technol. 298 (2022) 121542.
[15] O.A. Odunlami, D.A. Vershima, T.E. Oladimeji, S. Nkongho, S.K. Ogunlade, B. S. Fakinle, Advanced techniques for the capturing and separation of CO_2 – a review, Results Eng. 15 (2022) 100512.
[16] H. Rasool Abid, A. Keshavarz, J. Lercher, S. Iglauer, Promising material for large-scale H2 storage and efficient H2-CO2 separation, Sep. Purif. Technol. 298 (2022) 121542.
[17] U. Kamran, S.-J. Park, Chemically modified carbonaceous adsorbents for enhanced CO_2 capture: a review, J. Clean. Prod. 290 (2021) 125776.
[18] V. Katheresan, J. Kansedo, S.Y. Lau, Efficiency of various recent wastewater dye removal methods: a review, J. Environ. Chem. Eng. 6 (2018) 4676–4697.
[19] F. Alhammad, M. Ali, N. Yekeen, M. Ali, H.R. Abid, H. Hoteit, S. Iglauer, A. Keshavarz, Effect of methyl orange on the wettability of organic-acid-aged sandstone formations: implications for CO_2 geo-storage, Energy Fuel (2023).
[20] A. Škrjanc, M. Opresnik, M. Gabrijelčič, A. Šuligoj, G. Mali, N. Zabukovec Logar, Impact of dye encapsulation in ZIF-8 on CO_2, water, and wet CO_2 sorption, Molecules 28 (2023) 7056.
[21] H.R. Abid, S. Iglauer, A. Al-Yaseri, A. Keshavarz, Drastic enhancement of CO_2 adsorption capacity by negatively charged sub-bituminous coal, Energy 233 (2021) 120924.

[22] M.M. Rahman, M. Muttakin, A. Pal, A.Z. Shafiullah, B.B. Saha, A statistical approach to determine optimal models for IUPAC-classified adsorption isotherms, Energies 12 (2019) 4565.
[23] K. Sing, The use of nitrogen adsorption for the characterisation of porous materials, Colloids Surf. A Physicochem. Eng. Asp. 187 (2001) 3–9.
[24] K.A. Cychosz, R. Guillet-Nicolas, J. García-Martínez, M. Thommes, Recent advances in the textural characterization of hierarchically structured nanoporous materials, Chem. Soc. Rev. 46 (2017) 389–414.
[25] M. Sahimi, Flow and Transport in Porous Media and Fractured Rock: From Classical Methods to Modern Approaches, John Wiley & Sons, 2011.
[26] S. Zaboon, H.R. Abid, Z. Yao, R. Gubner, S. Wang, A. Barifcani, Removal of monoethylene glycol from wastewater by using Zr-metal organic frameworks, J. Colloid Interface Sci. 523 (2018) 75–85.
[27] D.C. Kalyani, A.A. Telke, S.P. Govindwar, J.P. Jadhav, Biodegradation and detoxification of reactive textile dye by isolated Pseudomonas sp. SUK1, Water Environ. Res. 81 (2009) 298–307.
[28] S. Yao, K. Zhang, K. Jiao, W. Hu, Evolution of coal structures: FTIR analyses of experimental simulations and naturally matured coals in the Ordos Basin, China, Energy Explor. Exploit. 29 (2011) 1–19.
[29] J. Coates, Interpretation of infrared spectra, a practical approach, Encyclopedia of Analytical Chemistry: Applications, Theory and Instrumentation, 2006.
[30] A. Tironi, M.A. Trezza, E.F. Irassar, A.N. Scian, Thermal treatment of kaolin: effect on the pozzolanic activity, Procedia Mater. Sci. 1 (2012) 343–350.
[31] R.M. Flores, Chapter 4 - coalification, gasification, and gas storage, in: R.M. Flores (Ed.), Coal and Coalbed Gas, Elsevier, Boston, 2014, pp. 167–233.
[32] S. Iglauer, H. Akhondzadeh, H. Abid, A. Paluszny, A. Keshavarz, M. Ali, A. Giwelli, L. Esteban, J. Sarout, M. Lebedev, Hydrogen flooding of a coal core: effect on coal swelling, Geophys. Res. Lett. 49 (2022), e2021GL096873.
[33] K.O. Iwuozor, J.O. Ighalo, E.C. Emenike, L.A. Ogunfowora, C.A. Igwegbe, Adsorption of methyl orange: a review on adsorbent performance, Curr. Res. Green Sustain. Chem. 4 (2021) 100179.
[34] R.L. Sweany, Metal Dihydrogen and σ-Bond Complexes: Structure, Theory, and Reactivity By Gregory J. Kubas, Los Alamos National Laboratory, Kluwer Academic/Plenum Publishers, New York, 2002, 2001. xvi+ 472 pp. $95.00. ISBN 0-306-46465-9, ACS Publications.
[35] G.E. Froudakis, Why alkali-metal-doped carbon nanotubes possess high hydrogen uptake, Nano Lett. 1 (2001) 531–533.
[36] Z. Zhang, Effect of External Electric Field on Hydrogen Adsorption Over Activated Carbon Separated by Dielectric Materials, 2012.
[37] M.D. Elola, J. Rodriguez, Preferential adsorption in ethane/carbon dioxide fluid mixtures confined within silica nanopores, J. Phys. Chem. C 123 (2019) 30937–30948.
[38] M. Arif, H. Rasool Abid, A. Keshavarz, F. Jones, S. Iglauer, Hydrogen storage potential of coals as a function of pressure, temperature, and rank, J. Colloid Interface Sci. 620 (2022) 86–93.
[39] D. Zhang, L. Gu, S. Li, P. Lian, J. Tao, Interactions of Supercritical CO_2 with coal, Energy Fuel 27 (2013) 387–393.
[40] M. Arjmandi, M. Pakizeh, An experimental study of H_2 and CO_2 adsorption behavior of C-MOF-5 and T-MOF-5: a complementary study, Braz. J. Chem. Eng. 33 (2016) 225–233.
[41] K.H. Kim, M.H. Kim, Adsorption of CO_2, CO, H_2, and N_2 on zeolites, activated carbons, and metal-organic frameworks with different surface nonuniformities, Sustainability 15 (2023) 11574.
[42] C.A. Grande, F.V.S. Lopes, A.M. Ribeiro, J.M. Loureiro, A.E. Rodrigues, Adsorption of off-gases from steam methane reforming (H_2, CO_2, CH_4, CO and N_2) on activated carbon, Sep. Sci. Technol. 43 (2008) 1338–1364.
[43] B. Yilmaz, N. Trukhan, U. MüLLER, Industrial outlook on zeolites and metal organic frameworks, Chin. J. Catal. 33 (2012) 3–10.
[44] Y.G. Chung, D.A. Gómez-Gualdrón, P. Li, K.T. Leperi, P. Deria, H. Zhang, N. A. Vermeulen, J.F. Stoddart, F. You, J.T. Hupp, O.K. Farha, R.Q. Snurr, In silico discovery of metal-organic frameworks for precombustion CO_2 capture using a genetic algorithm, Sci. Adv. 2 (2016), e1600909.
[45] H.R. Abid, A. Hanif, A. Keshavarz, J. Shang, S. Iglauer, CO_2, CH_4, and H_2 adsorption performance of the metal–organic framework HKUST-1 by modified synthesis strategies, Energy Fuel 37 (2023) 7260–7267.
[46] Z.R. Herm, J.A. Swisher, B. Smit, R. Krishna, J.R. Long, Metal–organic frameworks as adsorbents for hydrogen purification and precombustion carbon dioxide capture, J. Am. Chem. Soc. 133 (2011) 5664–5667.
[47] J. Hwang, H. Azzan, R. Pini, C. Petit, H_2, N_2, CO_2, and CH_4 unary adsorption isotherm measurements at low and high pressures on zeolitic imidazolate framework ZIF-8, J. Chem. Eng. Data 67 (2022) 1674–1686.
[48] A. Alanazi, H. Rasool Abid, M. Usman, M. Ali, A. Keshavarz, V. Vahrenkamp, S. Iglauer, H. Hoteit, Hydrogen, carbon dioxide, and methane adsorption potential on Jordanian organic-rich source rocks: implications for underground H_2 storage and retrieval, Fuel 346 (2023) 128362.
[49] A. Streb, M. Mazzotti, Adsorption for efficient low carbon hydrogen production: part 1—adsorption equilibrium and breakthrough studies for $H_2/CO_2/CH_4$ on zeolite 13X, Adsorption 27 (2021) 541–558.
[50] R.V. Siriwardane, M.-S. Shen, E.P. Fisher, J.A. Poston, Adsorption of CO2 on molecular sieves and activated carbon, Energy Fuel 15 (2001) 279–284.
[51] Y. Belmabkhout, A. Sayari, Adsorption of CO2 from dry gases on MCM-41 silica at ambient temperature and high pressure. 2: adsorption of CO_2/N_2, CO_2/CH_4 and CO_2/H_2 binary mixtures, Chem. Eng. Sci. 64 (2009) 3729–3735.